

STUDY ON SEISMIC GROUND MOTION OF P -WAVE INCIDENT ELASTIC FOUNDATION FREE FIELD UNDER THERMAL EFFECT

YIQI YANG

School of Civil Engineering, Qinghai University, Xining, China

QIANG MA

School of Civil Engineering, Qinghai University, Xining, China; and

Qinghai Provincial Key Laboratory of Energy-saving Building Materials and Engineering Safety, Xining, China

corresponding author Qiang Ma, e-mail: maqiang0104@163.com

This study extends the traditional problem of a seismic response of elastic foundations under isothermal conditions when considering thermal effects. Firstly, a free-field model of the elastic foundation is established under the incidence of plane P -waves. Then, utilizing the principles of wave propagation in a homogeneous and isotropic thermoelastic medium and the principle of Helmholtz vector decomposition, the influence of thermal physical parameters such as thermal conductivity, medium temperature on seismic ground motion of the free-field on elastic foundation is investigated, which provides a reasonable explanation for the ground motion of a site under thermal effects.

Keywords: single-phase thermoelastic medium, free field, seismic ground motion, plane P -wave

1. Introduction

The problem of a site seismic response, or the influence of site conditions on seismic wave propagation, has attracted much attention as one of the two major fluctuation problems in seismic engineering. The initial research on the seismic response problem of elastic foundations has been considering isothermal conditions. However, with the accelerated industrialization and modernization in various countries, the fields of petroleum engineering, pavement engineering, thermal engineering and chemical engineering are thriving. The impact of thermal effects, such as temperature fluctuations, on wave propagation characteristics in elastic media has garnered an increased attention of numerous scholars. Due to the mutual coupling between heat and force, the propagation of waves in elastic media is more complicated. Therefore, it is crucial to establish a free-field model that can reflect the actual site soil properties under non-isothermal conditions by considering thermal effects and studying seismic ground motion of the free field with elastic foundations.

The theory of uncoupled thermoelasticity was introduced by Duhamel (1837) and Neuman (1885), but it has two main limitations. The first limitation is that the theory assumes that the temperature does not affect the mechanical state of an elastomer, which does not follow the actual physical experiments. Secondly, the theory assumes that the propagation velocity of thermal waves is infinite, which is also physically unreasonable. Then Biot (1956) proposed the thermoelastic coupling theory, which resolves the first issue with the uncoupled theory, but unfortunately, the coupled theory still has the second limitation. To overcome this drawback, scholars proposed two generalized thermoelastic theories that allow thermal waves to propagate at finite velocities. Lord and Shulman (1967) introduced a new thermoelastic coupling theory to modify

Fourier's heat conduction theorem based on considering the effect of a flux-rate term, which allows prediction of finite velocities when thermal waves propagate. Green and Lindsay (1972) presented a generalized theory of thermoelasticity that modifies the Duhamel-Neumann relation and the energy balance equation. Based on previous studies, Green and Naghdi (1991) developed a novel thermodynamic model of deformed media, which explained the phenomenon of the thermal wave propagating at a finite speed in detail under the heat flow environment in rigid solids. Green and Naghdi (1993) then gave a detailed explanation and constructed a new thermoelasticity theory based on the thermodynamic model, which defined the heat flow as a heat wave propagating at a finite velocity. Tzou (1995a,b) introduced the heat flux phase delay time and temperature gradient phase delay time based on the previous studies to make corrections to Fourier's heat conduction theorem with a modification and proposed a two-phase lag model for single-phase thermoelastic media. Hetnarski and Ignaczak (1999) published a review paper on the representation within the scope of generalized thermoelasticity theory. Abouelregal (2011) presented basic control equations for generalized isotropic thermal elastomers without body forces and heat sources.

Scholars have extensively researched the propagation of thermoelastic waves in elastic media using the aforementioned generalized thermoelasticity theory. Sinha and Sinha (1974) as well as Sinha and Elsibai (1996, 1997) studied the reflection of thermoelastic waves at the interface of two semi-infinite media and from the free surface of a solid half-space, respectively. Abd-Alla and Al-Dawry (2000) explored the reflection phenomenon of SV waves in a thermoelastic medium. Sharma *et al.* (2003) investigated the problem of thermoelastic wave reflection from various boundaries of a solid half-space under different theories of generalized thermoelasticity. Furthermore, Singh (2005b) focused on the reflection of SV waves from the free surface of an elastic medium. Then Singh (2005a) went on to study the phenomenon of reflection of P and SV waves from the free surface of an elastic medium with thermal diffusion properties. Kumar and Sharma (2005) examined the reflection of a plane wave on a thermoelastic half-space boundary.

Although scholars at home and abroad have executed some studies on the propagation of thermoelastic waves in single-phase media and the reflection trouble on the interface of such media, there are few studies on seismic ground motion of a free field on a elastic foundation. Wang and Zhao (2022) studied the seismic response of subsurface structures in single-phase soils. Zhao *et al.* (2022) studied the seismic response of elastic foundations under the action of Rayleigh waves. However, previous studies have been on the seismic ground motion of the free field of elastic foundations under isothermal conditions. No papers have investigated the effect of the incident plane waves on the free field of elastic foundations on the seismic ground motion under thermal effects. However, the thermal effect significantly affects the wave propagation characteristics. The impact of heat on elastic wave propagation is related to numerous seismological and astrophysical issues, thereby holding far-reaching significance for researching seismic motion analysis of free sites considering the effect of heat. Moreover, this study offers a plausible explanation for the seismic ground motion of a site under the impact of heat and provides technical support for the seismic design of large structures in the area.

In this paper, based on the fluctuation equation of a single-phase thermoelastic medium established by Liu *et al.* (2021), the corresponding fluctuation equation of a thermoelastic medium is solved in the right-angle coordinate system. The free-field model of the elastic foundation is established, the wave field of the site is analyzed, and the analytical solution of each amplitude coefficient is obtained by combining the wave field function and the corresponding boundary conditions. Finally, the impact of thermal physical parameter such as medium temperature on the ground motion of the earthquake site is analyzed.

2. Field fluctuation equation for elastic media

Bedrock layers I and II are simulated with the use of a single-phase thermoelastic medium. According to the generalized thermoelasticity theory, the fluctuation equation for a single-phase thermoelastic medium was proposed (Liu *et al.*, 2021) as follows

$$\begin{aligned} \mu_e \nabla^2 \mathbf{u}^s + (\lambda_e + \mu_e) \nabla(\nabla \cdot \mathbf{u}^s) - 3K_b \beta_s \nabla T &= \rho^e \ddot{\mathbf{u}}^s \\ 3K_b \beta_s T_0 \nabla \cdot (\dot{\mathbf{u}}^s + \tau_{qe} \ddot{\mathbf{u}}^s t) + \rho^e c_{se} (\dot{T} + \tau_{qe} \ddot{T}) &= K_e \nabla^2 (T + \tau_{\theta e} \dot{T}) \end{aligned} \quad (2.1)$$

where $K_b = (\lambda_e + 2\mu_e)/3$ – bulk modulus, λ_e and μ_e – Lamé's constant of the single-phase medium, β_s – thermal expansion coefficient, ρ_e – density, c_{se} – specific heat capacity of the solid phase, τ_{qe} – phase-lag of the heat flux, $\tau_{\theta e}$ – phase-lag of the gradient of temperature, T – Kelvin medium temperature, T_0 – initial temperature, K_e – thermal conductivity, \mathbf{u}^s – solid phase displacement.

According to the decomposition principle of the Helmholtz vector, the solid phase displacement vector can be decomposed as follows

$$\mathbf{u}^s = \nabla \psi_s + \nabla \times \mathbf{H}^s \quad (2.2)$$

where ψ_s denotes the scalar potential function of the solid skeleton and \mathbf{H}^s denotes the vector potential function of the solid skeleton.

The potential function in a solid-phase medium can be assumed as

$$\begin{aligned} \psi^s &= A^s \exp[i(k_p x - \omega t)] & \mathbf{H}^s &= \mathbf{B}^s \exp[i(k_s x - \omega t)] \\ T &= A^T \exp[i(k_p x - \omega t)] \end{aligned} \quad (2.3)$$

where A^s and \mathbf{B}^s represent amplitudes of the corresponding potential functions, k_p denotes the complex wave number of P -wave (including T -wave), k_s denotes the complex wave number of S -wave, i denotes the imaginary number which satisfies $i = \sqrt{-1}$, ω is the angular frequency.

Substituting Eq. (2.2) into Equations (2.1) and then combining the resulting equations with Eqs. (2.3), the theoretical derivation leads to the characteristic equation for the bulk wave in a thermoelastic single-phase solid medium as follows

$$\begin{vmatrix} k_{11} & k_{12} \\ k_{21} & k_{22} \end{vmatrix} = 0 \quad |\rho^e \omega^2 - \mu_e k_s^2| = 0 \quad (2.4)$$

By solving characteristic equations (2.4), it is known that there are two compressional waves (containing thermal waves) and one shear wave in a single-phase thermoelastic medium.

3. Wavefield analysis

Consider a plane P -wave with a frequency of ω that is incident upon the interface between single-phase thermoelastic media I and II at an arbitrary angle φ , originating from the bedrock layer. The resulting wave propagates and generates three types of reflected waves (reflected P -, S - and T -wave) as well as three types of transmitted waves (transmitted P -, T - and S -wave) within both media. The entire process is depicted in Fig. 1. As the seismic wave continues to propagate in the elastic medium, the reflected P -, T - and S -wave are generated at the interface between the single-phase thermoelastic medium II and the free surface.

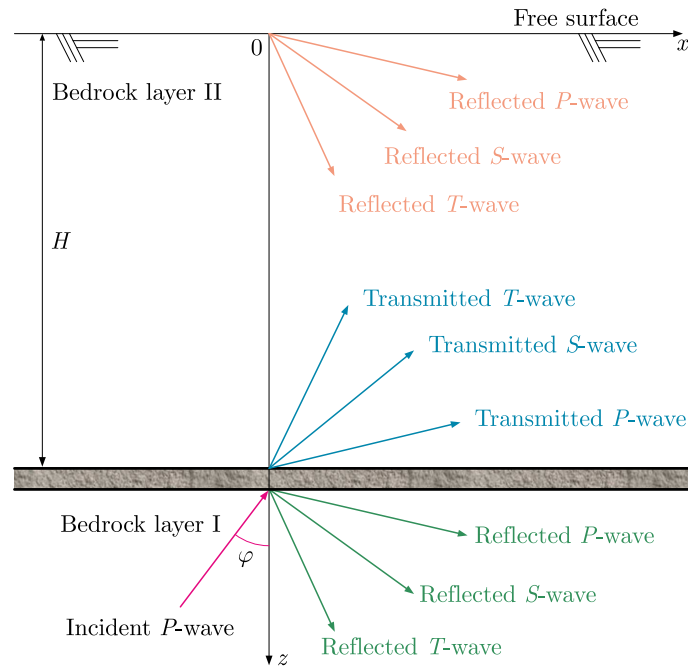


Fig. 1. Simplified model of the elastic foundation free field

3.1. Wave field functions and their solutions

The paper expresses the functional form of the wave field in both single-phase media I and II as follows:

(1) In bedrock layer I ($z > H$)

— P -wave

$$\begin{aligned} \psi^e &= A_{ip1}^s \exp[ik_{ip1}(l_{ip1}x - n_{ip1}z - c_{ip1}t)] \\ &+ \sum_{n=1}^2 A_{1rpn}^s \exp[ik_{1rpn}(l_{1rpn}x + n_{1rpn}z - c_{1rpn}t)] \end{aligned} \quad (3.1)$$

— T -wave

$$\begin{aligned} T^e &= A_{ip1}^s \delta_{Tp1}^e \exp[ik_{ip1}(l_{ip1}x - n_{ip1}z - c_{ip1}t)] \\ &+ \sum_{n=1}^2 A_{1rpn}^s \delta_{Tpn}^e \exp[ik_{1rpn}(l_{1rpn}x + n_{1rpn}z - c_{1rpn}t)] \end{aligned} \quad (3.2)$$

— S -wave

$$\mathbf{H}^e = \mathbf{B}_{1rs} \exp[ik_{1rs}(l_{1rs}x + n_{1rs}z - c_{1rs}t)] \quad (3.3)$$

(2) In bedrock layer II ($0 < z < H$)

— P -wave

$$\begin{aligned} \psi^u &= \sum_{n=1}^2 A_{tpn} \exp[ik_{tpn}(l_{tpn}x - n_{tpn}z - c_{tpn}t)] \\ &+ \sum_{n=1}^2 A_{2rpn} \exp[ik_{2rpn}(l_{2rpn}x + n_{2rpn}z - c_{2rpn}t)] \end{aligned} \quad (3.4)$$

— T -wave

$$T^u = \sum_{n=1}^2 A_{tpn}^s \delta_{Tpn}^u \exp[ik_{tpn}(l_{tpn}x - n_{tpn}z - c_{tpn}t)] + \sum_{n=1}^2 A_{2rpn}^s \delta_{Tpn}^u \exp[ik_{2rpn}(l_{2rpn}x + n_{2rpn}z - c_{2rpn}t)] \quad (3.5)$$

— S -wave

$$\mathbf{H}^u = \mathbf{B}_{2ts} \exp[ik_{2ts}(l_{2ts}x - n_{2ts}z - c_{2ts}t)] + \mathbf{B}_{2rs} \exp[ik_{2rs}(l_{2rs}x + n_{2rs}z - c_{2rs}t)] \quad (3.6)$$

where the subscripts i , r and t correspond to the incident, reflected and transmitted waves, respectively. β denotes different reflected P -wave (including T -wave) in single-phase medium I ($\beta = 1, 2$), and n denotes different reflected and transmitted P -wave (including T -wave) in single-phase medium II ($n = 1, 2$). k_{ip1} and c_{ip1} represent the wave number and velocity of the incident P -wave, respectively. $k_{1rp\beta}$ and k_{1rs} denote complex wave numbers of two reflected compressional waves (P -wave and T -wave) and one reflected shear wave (S -wave) in single-phase thermoelastic medium I, respectively. $c_{1rp\beta}$ and c_{1rs} denote wave velocities of the two reflected compressional waves (P -wave, T -wave) and one reflected shear wave (S -wave) in single-phase thermoelastic medium I, respectively. k_{tpn} and k_{2ts} represent wave numbers of the transmitted P -wave (including T -wave) and transmitted S -wave in single-phase thermoelastic medium II, respectively. c_{tpn} and c_{2ts} represent velocities of the transmitted P -wave (including T -wave) and transmitted S -wave in single-phase medium II. k_{2rpn} and k_{2rs} represent wave numbers of the reflected P -wave (including T -wave) and reflected S -wave in single-phase medium II, respectively. c_{2rpn} and c_{2rs} denote velocities of the reflected P -wave (including T -wave) and reflected S -wave in single-phase medium II, respectively. l , n denotes the direction vector of the corresponding wave.

According to Snell's theorem, in single-phase medium I and adjacent single-phase medium II, the number of waves in the horizontal direction of each bulk wave must be equal, as follows

$$l_{ip}k_{ip} = l_{1rp1}k_{1rp1} = l_{1rp2}k_{1rp2} = l_{1rs}k_{1rs} = l_{tp1}k_{tp1} = l_{tp2}k_{tp2} = l_{2ts}k_{2ts} \quad (3.7)$$

Upon taking the derivative of Eqs. (2.4), one arrives at the amplitude ratio of the potential function between the P -wave and T -wave in the single-phase thermoelastic medium:

$$\delta_{Tpn} = \frac{A_T}{A_S} = -\frac{k_{11}}{k_{12}} \quad n = 1, 2 \quad (3.8)$$

3.2. Boundary conditions

(1) The boundary conditions at the interface between single-phase thermoelastic media I and II ($z = H$) are as follows:

— stress continuity at the cross-interface

$$\sigma_{zz} = \sigma_{zz}^e \quad \sigma_{xz} = \sigma_{xz}^e \quad (3.9)$$

— the solid phase displacement at the interface is continuous

$$u_z^s = u_z^e \quad u_x^s = u_x^e \quad (3.10)$$

— temperature and its change rate at the interface are continuous

$$T = T^e \quad K \frac{\partial T}{\partial z} = K^e \frac{\partial T^e}{\partial z} \quad (3.11)$$

(2) At the interface between single-phase thermoelastic medium II and the free surface ($z = 0$), the following hold

$$\sigma_{zz} = 0 \quad \sigma_{xz} = 0 \quad \frac{\partial T}{\partial z} = 0 \quad (3.12)$$

The expression for the stress displacement in a single-phase medium is as follows

$$\begin{aligned} u_x &= \frac{\partial \psi^s}{\partial x} - \frac{\partial \mathbf{H}^s}{\partial z} & u_z &= \frac{\partial \psi^s}{\partial z} + \frac{\partial \mathbf{H}^s}{\partial x} \\ \sigma_{xz} &= \mu \left(2 \frac{\partial^2 \psi^s}{\partial x \partial z} + \frac{\partial^2 \mathbf{H}^s}{\partial x^2} - \frac{\partial^2 \mathbf{H}^s}{\partial z^2} \right) \\ \sigma_{zz} &= \lambda \left(\frac{\partial^2 \psi^s}{\partial x^2} + \frac{\partial^2 \psi^s}{\partial z^2} \right) + 2\mu^e \left(\frac{\partial^2 \psi^s}{\partial z^2} + \frac{\partial^2 \mathbf{H}^s}{\partial x \partial z} \right) - 3K_b \beta_T T \end{aligned} \quad (3.13)$$

The wave field functions Eqs. (3.1) to (3.3) and Eqs. (3.4) to (3.6) are substituted into the boundary conditions Eqs. (3.9) to (3.11) and (3.12) to obtain each amplitude coefficient, which may be represented as a system of linear equations

$$\mathbf{FN} = A_{ip} \mathbf{G} \quad (3.14)$$

where $\mathbf{N} = [A_{1rp1}^s, A_{1rp2}^s, B_{1rs}^s, A_{tp1}^s, A_{tp2}^s, B_{2ts}^s, A_{2rp1}^s, A_{2rp2}^s, B_{2rs}^s]^T$, the elements f_{11} - f_{99} and g_{1} - g_{9} in the matrix are given in Appendix A.

4. Free surface displacement

Upon determining the wave field, it is possible to calculate the displacement and stress on the site. By substituting Eqs. (3.4)-(3.6) into the relevant expression, the expressions for surface displacement U_x and U_z can be obtained

$$\begin{aligned} U_x &= A_{tp1}^s i k_{tp1} l_{tp1} + A_{tp2}^s i k_{tp2} l_{tp2} + A_{2rp1}^s i k_{2rp1} l_{2rp1} + A_{2rp2}^s i k_{2rp2} l_{2rp2} \\ &\quad + B_{2ts}^s i k_{2ts} n_{2ts} - B_{2rs}^s i k_{2rs} n_{2rs} \\ U_z &= -A_{tp1}^s i k_{tp1} n_{tp1} - A_{tp2}^s i k_{tp2} n_{tp2} + A_{2rp1}^s i k_{2rp1} n_{2rp1} + A_{2rp2}^s i k_{2rp2} n_{2rp2} \\ &\quad + B_{2ts}^s i k_{2ts} l_{2ts} + B_{2rs}^s i k_{2rs} l_{2rs} \end{aligned} \quad (4.1)$$

In this paper, the displacement amplification coefficients u_x/u_0 and u_z/u_0 of the free-field surface are used to characterize the surface displacement of the elastic foundation free-field, where the displacement amplification coefficient is expressed as the ratio of the displacement amplitude in the corresponding direction to the displacement amplitude of the incident wave u_0 .

5. Numerical analysis

Through numerical calculations, the P -wave incident elastic foundation free site seismic ground motion under the thermal effects is studied, and the impact of parameters such as medium temperature, on seismic ground motion produced by the site are specifically analyzed. Among them, the material parameters of the single-phase thermoelastic medium are chosen according to Liu *et al.* (2021). Table 1 illustrates the necessary parameters for numerical simulations.

Table 1. Physical parameters of single-phase thermoelastic media

Material parameters						
Thermal conductivity K_e [J/s/m/K]	Density of soil particle ρ^e [Kg/m ³]	Solid phase heat c_{se} [J/kg/K]	Phase lag of the heat flux τ_{qe} [s]	Phase lag of gradient of temperature $\tau_{\theta e}$ [s]	Medium temperature T [K]	Thermal expansion coefficient β_{Te} [1/K]
3	2700	1046	$2.0 \cdot 10^{-7}$	$1.5 \cdot 10^{-7}$	293.2	$4.0 \cdot 10^{-4}$
Lamé constant λ_e [kPa]	Lamé constant μ^e [kPa]	Thermal conductivity K^u [[J/s/m/K]	The density of soil particle ρ^u [Kg/m ³]	Solid phase heat c_{ue} [J/kg/K]	Phase lag of heat flux τ_{qu} [s]	Phase lag of gradient of temperature $\tau_{\theta u}$ [s]
$12 \cdot 10^6$	$8 \cdot 10^6$	3	2700	1046	$2.0 \cdot 10^{-7}$	$1.5 \cdot 10^{-7}$
Medium temperature T [K]	Thermal expansion coefficient β_{Tu} [1/K]	Lamé constant λ^u [kPa]	Lamé constant μ^u [kPa]			
293.2	$4.0 \cdot 10^{-4}$	$9 \cdot 10^6$	$4 \cdot 10^6$			

5.1. Effect of thermal conductivity at different incident angles

As is commonly understood, the magnitude of thermal conductivity is indicative of the soil capacity for heat transmission. A higher thermal conductivity results in more intense atomic thermal motion and faster propagation of heat. Conversely, a lower thermal conductivity leads to slower atomic thermal motion and slower propagation of heat. To investigate the regularity of how changes in thermal conductivity affect the amplification coefficient of surface displacement, one must keep other parameters constant. Figure 2 illustrates the curves depicting the surface displacement amplification coefficient as a function of the angle of incidence for varying levels of thermal conductivity. Firstly, observing Fig. 2, it is apparent that the horizontal and vertical

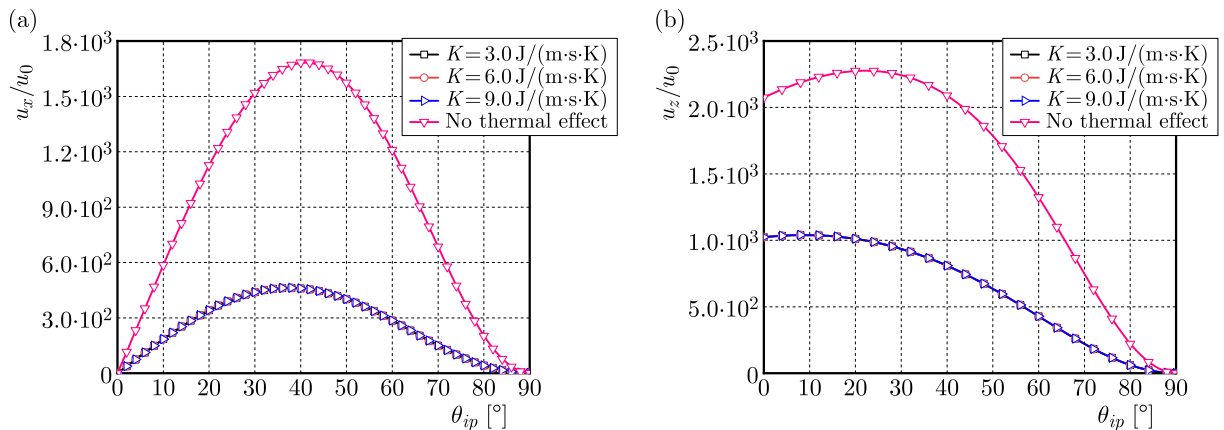


Fig. 2. Variation curve of the surface displacement amplification coefficient with the incident angle under different thermal conductivity

displacement amplification coefficients obtained for the two theoretical models considering the thermal effect and the other neglecting it have significant differences. When considering the thermal effect, the horizontal displacement amplification coefficient is similar to that without the thermal effect. However, the horizontal displacement amplification coefficient is smaller with the thermal effect. In the case of the vertical displacement amplification coefficient, both the

peak angle and the magnitude of the amplification coefficient are lower when thermal effects are considered. Furthermore, as depicted in Fig. 2, when taking thermal effects into account, both surface displacement amplification coefficients increase first and then decrease with a rise in the incidence angle. The horizontal and vertical displacement amplification coefficients reach the peak at the incidence angle $\varphi = 40^\circ$ and $\varphi = 15^\circ$, respectively. As the thermal conductivity increases, the surface displacement amplification coefficients undergo tiny changes. Thus, it is clear that the influence of considering thermal effects on the surface displacement amplification coefficient should not be disregarded.

5.2. Effect of thermal expansion coefficient at different incidence angles

To examine the influence of variations in thermal expansion coefficients on amplification coefficients of surface displacement, the other parameters are kept constant. Figure 3 displays the curves of the latter as a function of the incidence angle for varying levels of thermal expansion coefficients. Firstly, observing Fig. 3 that regardless of the value of the thermal expansion coefficient, when the P -wave is incident horizontally from the bedrock layer, the surface horizontal and vertical displacement amplification coefficients will be 0. The reason is that since the incident P -wave propagates in the horizontal direction, the transmission and reflection in single-phase medium II will disappear. That is, the free surface will not produce displacement. In addition, as the incident angle increases, the surface displacement amplification coefficients increase and then decrease, reaching the peak at the incident $\varphi = 40^\circ$ and $\varphi = 15^\circ$, respectively. Secondly, it can be found from Fig. 3 that with an increase in the thermal expansion coefficient, both the surface horizontal and vertical displacement amplification coefficient gradually decrease. As the incidence angle shifts, the impact of thermal expansion coefficients on the amplification coefficient of surface displacement becomes notably significant and thus cannot be dismissed.

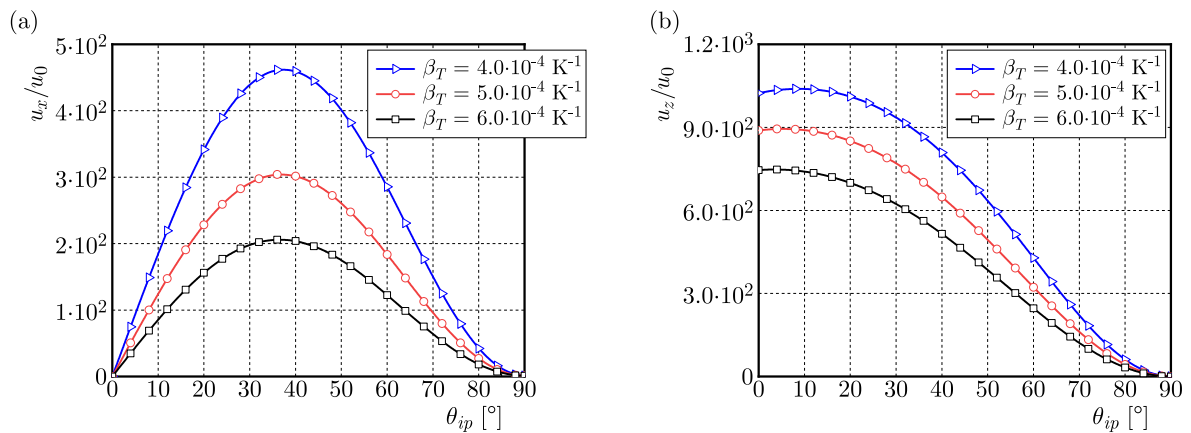


Fig. 3. Variation curve of the surface displacement amplification coefficient with the incident angle under different thermal expansion coefficient

5.3. Effect of medium temperature at different incidence angles

To investigate the impact of changing medium temperature on the displacement amplification coefficient of the ground surface, the other parameters are kept constant. Figure 4 illustrates how the amplification coefficient of ground surface displacement varies with the incidence angle for varying medium temperature levels. Firstly, observing Fig. 4, no matter what value the medium temperature takes with a change of the incident angle, the trend of the horizontal and vertical displacement amplification coefficient is the same. That is to say, with an increase in the incident angle, the displacement amplification of both factors increase first and then decrease, reaching the peak at the incident angle $\varphi = 40^\circ$ and $\varphi = 15^\circ$, respectively. Furthermore, it

is evident from Fig. 4 that the horizontal and vertical displacement amplification coefficient gradually decrease with a rise in medium temperature. It is apparent that changes in medium temperature significantly affect the ground displacement amplification coefficient as the incidence angle varies, and thus cannot be disregarded.

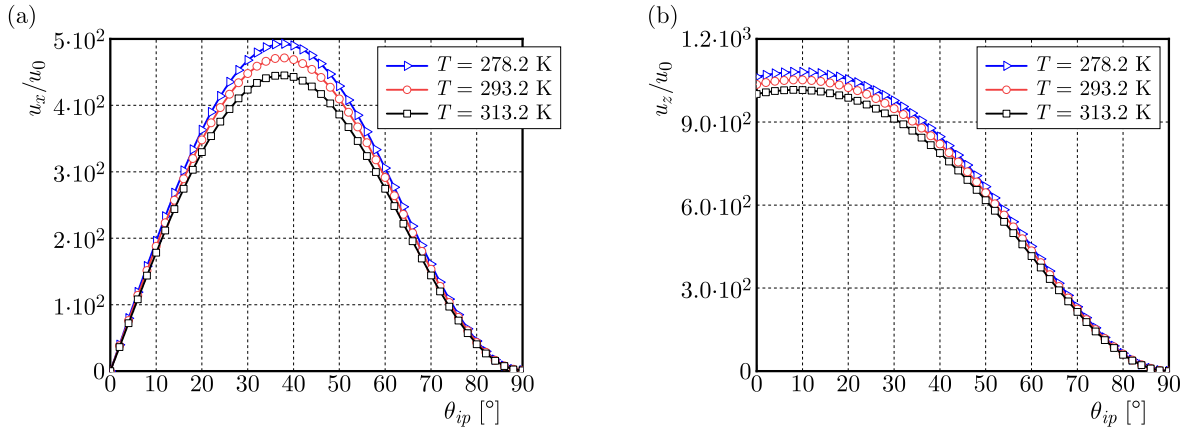


Fig. 4. Curves of the surface displacement amplification coefficient with the incident angle at different medium temperatures

5.4. Effect of the phase lag of the heat flux at different incidence angles

Compared the porous medium theory under isothermal conditions with thermoelastic theory, the T -wave will be generated. The phase lag of the heat flux plays a vital role in determining the fluctuation Eq. (2.1)₂ of the T -wave, and subsequently, affects its velocity. To investigate the influence of changes in the phase lag of the heat flux on the surface displacement amplification coefficient, the other parameters remain constant. Figure 5 displays the curves of the latter as a function of the incident angle for varying levels of the phase lag of the heat flux. Firstly, observing

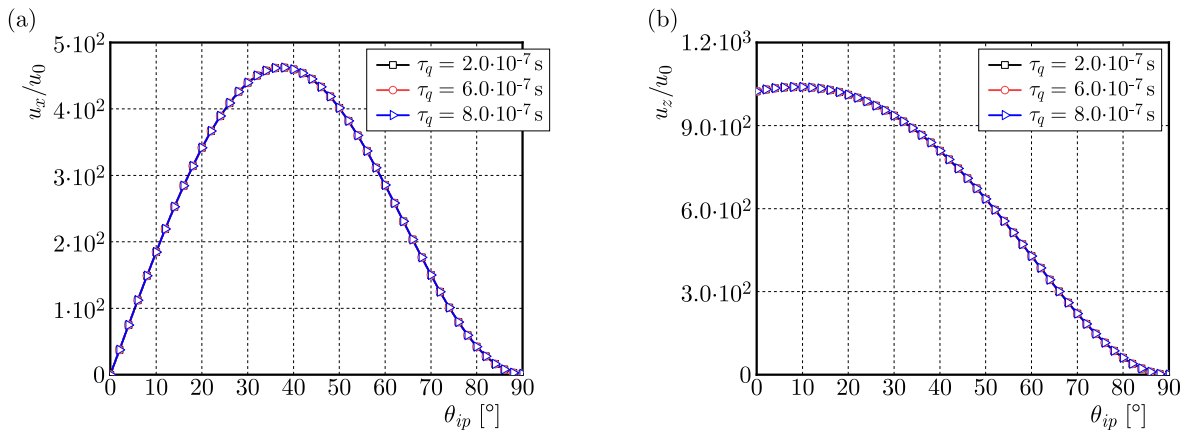


Fig. 5. The variation curve of the surface displacement amplification coefficient with the incidence angle under different phase lag of the heat flux

Fig. 5, both surface displacement amplification coefficients increase first and then decrease with a rise in the incidence angle and reach the peak at $\varphi = 40^\circ$ and $\varphi = 15^\circ$, respectively. Furthermore, it is evident from Fig. 5 that the horizontal and vertical displacement amplification coefficients just change slightly with an increase in the phase lag of the heat flux. According to the literature (Liu *et al.*, 2021), the change of the phase lag of the heat flux only affects the wave velocity of the T -wave but has little effect on the P -, S -wave. The velocity of the T -wave are several orders of magnitude lower than that of the P -, S -wave, so the horizontal and vertical displacement

amplification coefficients only change slightly with a rise in the phase lag of the heat flux, which also proves the correctness of the results in this paper. Observing Fig. 5, it becomes apparent that changes in the phase lag of the heat flux have a negligible impact on the surface displacement amplification factors as the incident angle is varied.

5.5. Effect of incident frequency at different incidence angles

To analyze the impact of altering the incident frequency on the amplification coefficient of surface displacement, the other parameters are constant. Figure 6 displays the relationship curves between the surface displacement amplification coefficient and incident angle as the frequency ω increases from 5 Hz to 15 Hz, 30 Hz, and finally 50 Hz. Upon initial observation of Fig. 6, it is apparent that both surface displacement amplification coefficients increase first and then decrease with a rise in the incidence angle. The horizontal and vertical displacement amplification coefficients reach the peak at the incidence angle $\varphi = 40^\circ$ and $\varphi = 15^\circ$, respectively. Furthermore, it can be observed from Fig. 6 that both the horizontal and vertical displacement amplification coefficients increase with a rise in the incident frequency, and the magnitude of the increase in displacement amplitude increases continuously. It can be seen that the effect of considering the change of incident frequency on the surface displacement amplification coefficient is not negligible.

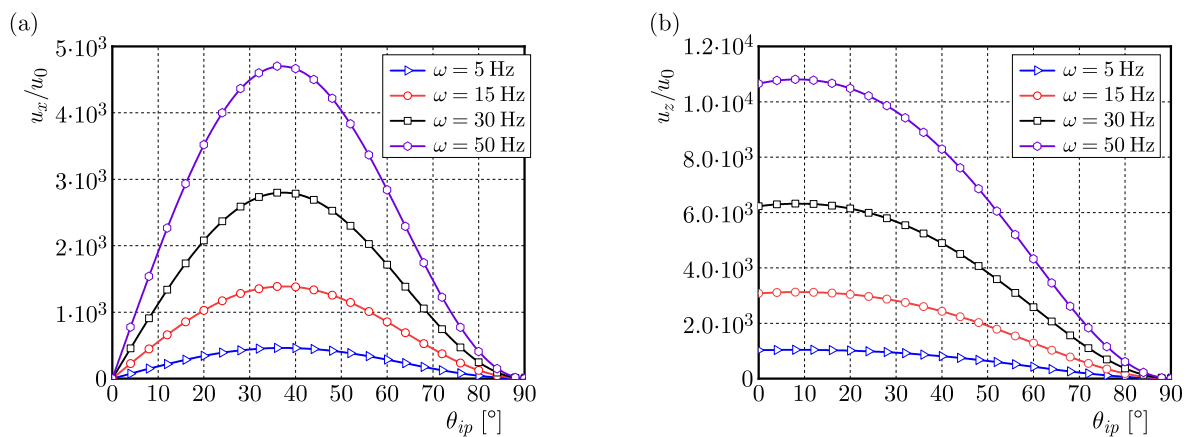


Fig. 6. The variation curve of the surface displacement amplification coefficient with the incidence angle under different incident frequencies

6. Conclusion

Based on the wave propagation theory in single-phase thermoelastic media, this paper studies seismic ground motion of the free field on an elastic foundation under a plane P -wave incidence. The influence of thermal physical parameters such as medium temperature on the seismic ground motion of the site is analyzed. The results indicate that:

- Significant differences are evident between the surface displacement amplification coefficients obtained under two theoretical models – one considering thermal effects and the other neglecting them.
- The surface displacement amplification coefficients decrease as the thermal expansion coefficient and medium temperature increase when the plane P -wave is incident upon the elastic foundation free-field under the thermal effects. The phase lag of the heat flux has a negligible impact on the surface displacement amplification coefficient.
- With a rise in the incident frequency, the surface displacement amplification coefficients gradually increase, and the amplitude of the increase becomes larger and larger.

Appendix A

$$\begin{aligned}
f_{11} &= [-(\lambda^e + 2\mu^e n_{1rp1}^2)k_{1rp1}^2 - 3K_b^e \beta_T^e \delta_{TP1}^e] \exp(ik_{1rp1}n_{1rp1}H) \\
f_{12} &= [-(\lambda^e + 2\mu^e n_{1rp2}^2)k_{1rp2}^2 - 3K_b^e \beta_T^e \delta_{TP2}^e] \exp(ik_{1rp2}n_{1rp2}H) \\
f_{13} &= -2\mu^e l_{1rs}n_{1rs}k_{1rs}^2 \exp(ik_{1rs}n_{1rs}H) \\
f_{14} &= [(\lambda^u + 2\mu^u n_{tp1}^2)k_{tp1}^2 + 3K_b^u \beta_T^u \delta_{TP1}^u] \exp(-ik_{tp1}n_{tp1}H) \\
f_{15} &= [(\lambda^u + 2\mu^u n_{tp2}^2)k_{tp2}^2 + 3K_b^u \beta_T^u \delta_{TP2}^u] \exp(-ik_{tp2}n_{tp2}H) \\
f_{16} &= -2\mu^u l_{2ts}n_{2ts}k_{2ts}^2 \exp(-ik_{2ts}n_{2ts}H) \\
f_{17} &= [(\lambda^u + 2\mu^u n_{2rp1}^2)k_{2rp1}^2 + 3K_b^u \beta_T^u \delta_{TP1}^u] \exp(ik_{2rp1}n_{2rp1}H) \\
f_{18} &= [(\lambda^u + 2\mu^u n_{2rp2}^2)k_{2rp2}^2 + 3K_b^u \beta_T^u \delta_{TP2}^u] \exp(ik_{2rp2}n_{2rp2}H) \\
f_{19} &= 2\mu^u l_{2rs}n_{2rs}k_{2rs}^2 \exp(ik_{2rs}n_{2rs}H) \\
f_{21} &= 2\mu^e l_{1rp1}n_{1rp1}k_{1rp1}^2 \exp(ik_{1rp1}n_{1rp1}H) & f_{22} &= 2\mu^e l_{1rp2}n_{1rp2}k_{1rp2}^2 \exp(ik_{1rp2}n_{1rp2}H) \\
f_{23} &= \mu^e (l_{1rs}^2 - n_{1rs}^2)k_{1rs}^2 \exp(ik_{1rs}n_{1rs}H) & f_{24} &= 2\mu^u l_{tp1}n_{tp1}k_{tp1}^2 \exp(-ik_{tp1}n_{tp1}H) \\
f_{25} &= 2\mu^u l_{tp2}n_{tp2}k_{tp2}^2 \exp(-ik_{tp2}n_{tp2}H) & f_{26} &= \mu(n_{2ts}^2 - l_{2ts}^2)k_{2ts}^2 \exp(-ik_{2ts}n_{2ts}H) \\
f_{27} &= -2\mu^u l_{2rp1}n_{2rp1}k_{2rp1}^2 \exp(ik_{2rp1}n_{2rp1}H) \\
f_{28} &= -2\mu^u l_{2rp2}n_{2rp2}k_{2rp2}^2 \exp(ik_{2rp2}n_{2rp2}H) \\
f_{29} &= \mu^u (n_{2rs}^2 - l_{2rs}^2)k_{2rs}^2 \exp(ik_{2rs}n_{2rs}H) & f_{31} &= n_{1rp1}k_{1rp1} \exp(ik_{1rp1}n_{1rp1}H) \\
f_{32} &= n_{1rp2}k_{1rp2} \exp(ik_{1rp2}n_{1rp2}H) & f_{33} &= l_{1rs}k_{1rs} \exp(ik_{1rs}n_{1rs}H) \\
f_{34} &= n_{tp1}k_{tp1} \exp(-ik_{tp1}n_{tp1}H) & f_{35} &= n_{tp2}k_{tp2} \exp(-ik_{tp2}n_{tp2}H) \\
f_{36} &= -l_{2ts}k_{2ts} \exp(-ik_{2ts}n_{2ts}H) & f_{37} &= -n_{2rp1}k_{2rp1} \exp(ik_{2rp1}n_{2rp1}H) \\
f_{38} &= -n_{2rp2}k_{2rp2} \exp(ik_{2rp2}n_{2rp2}H) & f_{39} &= -l_{2rs}k_{2rs} \exp(ik_{2rs}n_{2rs}H) \\
f_{41} &= -l_{1rp1}k_{1rp1} \exp(ik_{1rp1}n_{1rp1}H) & f_{42} &= -l_{1rp2}k_{1rp2} \exp(ik_{1rp2}n_{1rp2}H) \\
f_{43} &= n_{1rs}k_{1rs} \exp(ik_{1rs}n_{1rs}H) & f_{44} &= l_{tp1}k_{tp1} \exp(-ik_{tp1}n_{tp1}H) \\
f_{45} &= l_{tp2}k_{tp2} \exp(-ik_{tp2}n_{tp2}H) \\
f_{46} &= n_{2ts}k_{2ts} \exp(-ik_{2ts}n_{2ts}H) & f_{47} &= l_{2rp1}k_{2rp1} \exp(ik_{2rp1}n_{2rp1}H) \\
f_{48} &= l_{2rp2}k_{2rp2} \exp(ik_{2rp2}n_{2rp2}H) & f_{49} &= -n_{2rs}k_{2rs} \exp(ik_{2rs}n_{2rs}H) \\
f_{51} &= -\delta_{TP1}^e \exp(ik_{1rp1}n_{1rp1}H) & f_{52} &= -\delta_{TP2}^e \exp(ik_{1rp2}n_{1rp2}H) & f_{53} &= 0 \\
f_{54} &= \delta_{TP1}^u \exp(-ik_{tp1}n_{tp1}H) & f_{55} &= \delta_{TP2}^u \exp(-ik_{tp2}n_{tp2}H) & f_{56} &= 0 \\
f_{57} &= \delta_{TP1}^u \exp(ik_{2rp1}n_{2rp1}H) & f_{58} &= \delta_{TP2}^u \exp(ik_{2rp2}n_{2rp2}H) & f_{59} &= 0 \\
f_{61} &= K^e n_{1rp1}k_{1rp1} \delta_{TP1}^e \exp(ik_{1rp1}n_{1rp1}H) & f_{62} &= K^e n_{1rp2}k_{1rp2} \delta_{TP2}^e \exp(ik_{1rp2}n_{1rp2}H) \\
f_{63} &= 0 & f_{64} &= K^u n_{tp1}k_{tp1} \delta_{TP1}^u \exp(-ik_{tp1}n_{tp1}H) \\
f_{65} &= K^u n_{tp2}k_{tp2} \delta_{TP2}^u \exp(-ik_{tp2}n_{tp2}H) & f_{66} &= 0 \\
f_{67} &= -K^u n_{2rp1}k_{2rp1} \delta_{TP1}^u \exp(ik_{2rp1}n_{2rp1}H) \\
f_{68} &= -K^u n_{2rp2}k_{2rp2} \delta_{TP2}^u \exp(ik_{2rp2}n_{2rp2}H) & f_{69} &= 0 & f_{71} &= f_{72} = f_{73} = 0 \\
f_{74} &= (\lambda^u + 2\mu^u n_{tp1}^2)k_{tp1}^2 + 3K_b^u \beta_T^u \delta_{TP1}^u & f_{75} &= (\lambda^u + 2\mu^u n_{tp2}^2)k_{tp2}^2 + 3K_b^u \beta_T^u \delta_{TP2}^u \\
f_{76} &= -2\mu^u l_{2ts}n_{2ts}k_{2ts}^2 & f_{77} &= (\lambda^u + 2\mu^u n_{2rp1}^2)k_{2rp1}^2 + 3K_b^u \beta_T^u \delta_{TP1}^u \\
f_{78} &= (\lambda^u + 2\mu^u n_{2rp2}^2)k_{2rp2}^2 + 3K_b^u \beta_T^u \delta_{TP2}^u & f_{79} &= 2\mu^u l_{2rs}n_{2rs}k_{2rs}^2 \\
f_{81} &= f_{82} = f_{83} = 0 & f_{84} &= 2\mu^u l_{tp1}n_{tp1}k_{tp1}^2 & f_{85} &= 2\mu^u l_{tp2}n_{tp2}k_{tp2}^2 \\
f_{86} &= \mu^u (n_{2ts}^2 - l_{2ts}^2)k_{2ts}^2 & f_{87} &= -2\mu^u l_{2rp1}n_{2rp1}k_{2rp1}^2 \\
f_{88} &= -2\mu^u l_{2rp2}n_{2rp2}k_{2rp2}^2 & f_{89} &= \mu^u (n_{2rs}^2 - l_{2rs}^2)k_{2rs}^2 & f_{91} &= f_{92} = f_{93} = 0
\end{aligned}$$

$$\begin{aligned}
f_{94} &= n_{ip1}^2 k_{ip1}^2 \delta_{Tp1}^u & f_{95} &= n_{ip2}^2 k_{ip2}^2 \delta_{Tp2}^u & f_{96} &= 0 \\
f_{97} &= n_{2rp1}^2 k_{2rp1}^2 \delta_{Tp1}^u & f_{98} &= n_{2rp2}^2 k_{2rp2}^2 \delta_{Tp2}^u & f_{99} &= 0 \\
g_1 &= (\lambda^e + 2\mu^e n_{ip1}^2) k_{ip1}^2 \exp(-ik_{ip1} n_{ip1} H) + 3K_b^e \beta_T^e \delta_{Tp1}^e \exp(-ik_{ip1} n_{ip1} H) \\
g_2 &= 2\mu^e l_{ip1} n_{ip1} k_{ip1}^2 \exp(-ik_{ip1} n_{ip1} H) & g_3 &= k_{ip1} n_{ip1} \exp(-ik_{ip1} n_{ip1} H) \\
g_4 &= l_{ip1} k_{ip1} \exp(-ik_{ip1} n_{ip1} H) & g_5 &= \delta_{Tp1}^e \exp(-ik_{ip1} n_{ip1} H) \\
g_6 &= K^e n_{ip1} k_{ip1} \delta_{Tp1}^e \exp(-ik_{ip1} n_{ip1} H) & g_{7(1)} &= g_{8(1)} = g_{9(1)} = 0
\end{aligned}$$

Acknowledgments

The authors gratefully acknowledge the financial support of the Qinghai Province Science and Technology Department Project (No. 2021-ZJ-943Q) and the Chinese Natural Science Foundation (Grant No. 52168053).

References

1. ABD-ALLA A.N., AL-DAWY A.A.S., 2000, The reflection phenomena of SV-waves in a generalized thermoelastic medium, *International Journal of Mathematics and Mathematical Sciences*, **23**, 529-546
2. ABOUELREGAL A.E., 2011, Rayleigh waves in a thermoelastic solid half space using dual-phase-lag model, *International Journal of Engineering Science*, **49**, 781-791
3. BIOT M.A., 1956, Thermoelasticity and irreversible thermodynamics, *Journal of Applied Physics*, **27**, 240-253
4. DUHAMEL J., 1837, Some memoire sur les phenomenes phenomenon thermo-mechanique, *Journal de l'Ecole Polytechnique*, **15**
5. GREEN A.E., LINDSAY K.A., 1972, Thermoelasticity, *Journal of Elasticity*, **2**, 1-7
6. GREEN A.E., NAGHDI P.M., 1991, A re-examination of the basic postulates of thermomechanics, *Proceedings: Mathematical and Physical Sciences*, **432**, 1885
7. GREEN A.E., NAGHDI P.M., 1993, Thermoelasticity without energy dissipation, *Journal of Elasticity*, **31**, 189-208
8. HETNARSKI R.B., IGNACZAK J., 1999, Generalized thermoelasticity, *Journal of Thermal Stresses*, **22**, 451-476
9. KUMAR R., SHARMA J.N., 2005, Reflection of plane waves from the boundaries of a micropolar thermoelastic half-space without energy dissipation, *International Journal of Applied Mechanics and Engineering*, **10**, 4
10. LIU H.B., DAI G.L., ZHOU F.X., MU Z.L., 2021, Propagation behavior of homogeneous plane-P1-wave at the interface between a thermoelastic solid medium and an unsaturated porothermoelastic medium, *The European Physical Journal Plus*, **136**, 1163
11. LORD H.W., SHULMAN Y., 1967, A generalized dynamical theory of thermoelasticity, *Journal of the Mechanics and Physics of Solids*, **15**, 299-309
12. NEUMANN F., 1885, *Vorlesungen Uber die Theorie der Elasticitat*, Meyer: Brestau
13. SHARMA J.N., KUMAR V., CHAND D., 2003, Reflection of generalized thermoelastic waves from the boundary of a half-space, *Journal of Thermal Stresses*, **26**, 925-942
14. SINGH B., 2005a, Reflection of P and SV waves from free surface of an elastic solid with generalized thermodiffusion, *Journal of Earth System Science*, **114**, 2
15. SINGH B., 2005b, Reflection of SV waves from the free surface of an elastic solid in generalized thermoelastic diffusion, *Journal of Sound and Vibration*, **291**, 3-5, 764-778

16. SINHA A.N., SINHA S.B., 1974, Reflection of thermoelastic waves at a solid half-space with thermal relaxation, *Journal of Physics of the Earth*, **22**, 237-244
17. SINHA S.B., ELSIBAI K.A., 1996, Reflection of thermoelastic waves at a solid half-space with two relaxation times, *Journal of Thermal Stresses*, **19**, 749-762
18. SINHA S.B., ELSIBAI K.A., 1997. Reflection and refraction of thermoelastic waves at an interface of two semi-infinite media with two relaxation times, *Journal of Thermal Stresses*, **20**, 129-146
19. TZOU D.Y., 1995a, A unified field approach for heat conduction from macro- to micro-scales, *Journal of Heat Transfer*, **117**, 1, 8-16
20. TZOU D.Y., 1995b, Experimental support for the lagging behavior in heat propagation, *Journal of Thermophysics and Heat Transfer*, **9**, 4, 686-693
21. WANG X.B., ZHAO F., 2022, Comparative study of seismic response of subsurface structures in single-phase soils and saturated soil, *Sichuan Cement*, **3**, 22-23+26
22. ZHAO W.S., CHEN W.Z., YANG D.S., GAO H., XIE P.Y., 2022, Analytical solution for seismic response of tunnels with composite linings in elastic ground subjected to Rayleigh waves, *Soil Dynamics and Earthquake Engineering*, **153**, 107113

Manuscript received May 16, 2023; accepted for print June 26, 2023